

# Experimental investigation and applications of the modulational wave train

Takuji Waseda

Dept. Environmental and Ocean Engineering, University of Tokyo

## INTRODUCTION

The rapid decrease of the depth of the surrounding sea and the presence of the Kuroshio makes it extremely challenging for the exploration of marine resources near Japan. The country relies on a sustained physical distribution system on sea, and therefore the safety of the sea transportation is crucial. The University of Tokyo and the National Maritime Research Institute have initiated a research initiative to establish a ship avoidance system from the extreme seas. The 3-year project was initiated in 2004 in support of the grant-in-aid for scientific research (A) of the Japan Society for the Promotion of Science (JSPS). The effort is two-fold, the first group focuses on the mechanisms, detection and numerical simulation of the freak wave (Tomita NMRI, Kinoshita, Waseda, Kawamura, Rheem UT) and the second group focuses on the study of extreme wave loads on ships and design of an avoidance system (Yuhara, Suzuki, Yamato, Kagemoto UT, Tanizawa NMRI, Miyake NK). The research effort includes: wave generation, radar experiments in tanks, numerical simulations, analyses of marine accident records and designing a ship avoidance system. In this presentation, recent work on the wave generation in the tank will be reported.

## FACILITY

Ocean Engineering Tank of the Institute of Industrial Science of the University of Tokyo (Kinoshita laboratory and Rheem laboratory) is 50 m long, 10 m wide and 5 m deep. The tank (figure 1) is equipped with a towing carriage, a wind carriage, a multi-directional wave maker, and current generator. The multi-directional wave maker has thirty-two 31 cm-wide triangular plungers that are computer controlled in such a manner to generate waves of various periods (0.5 ~ 5 s) propagating at prescribed angles. Regular as well as irregular directional waves can be generated. The tank water can be circulated to generate constant current at a maximum speed of 0.2 m s<sup>-1</sup>.

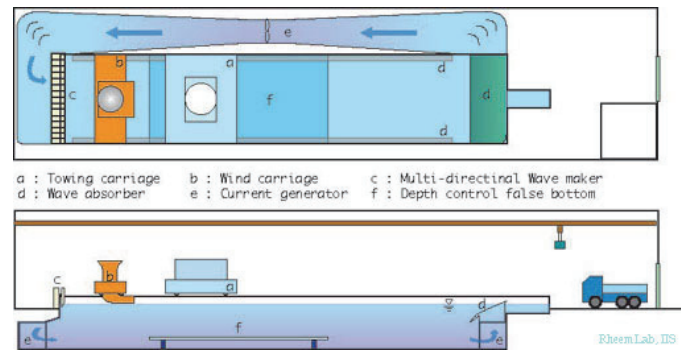


Figure 1: The Ocean Engineering Tank, Institute of Industrial Science of the University of Tokyo

## EXTREME WAVES IN TANK

The one-dimensional extreme waves generated so far are:

- i) Linear focusing wave + regular wave
- ii) Solitary wave group
- iii) BF instability wave train

The linear focusing wave is generated by a chirped time series. The rate of frequency modulation is determined based on geometrical optics approximation but because both the diffraction and non-linearity becomes important in the vicinity of the focal point, careful adjustment of the envelope shape was made so that the energy is concentrated at a single wave peak. Combination of the focusing wave and the regular wave train allows us to control the ratio of the background wave amplitude and the extreme wave. Further detail can be found in Waseda et al. (2005).

Solitary wave groups are generated as well. The motion of the wave generator is modulated following the envelope amplitude given by the exact analytical solution adjusted for the efficiency and the phase delay of the wave generator. The breather soliton (Ma-soliton) is generated in a similar manner. For the former case, the amplitude cannot be too high because the weak-nonlinear approximation becomes immediately violated and the waves break right after the waves are generated. The Ma-soliton is a better method to generate extreme wave since initially the solitary wave envelope amplitude is low. The Ma-soliton has been studied by Ten and Tomita (2005) in more detail where they compared the tank experiment and the fully-nonlinear numerical simulation.

The Benjamin-Feir instability wave train has been studied most extensively and was used for the radar experiment as well as the ship model testing. Following the earlier work by Tulin and Waseda (1999) parameter space  $\varepsilon$ - $\delta$  was explored, where  $\varepsilon$  is the initial steepness of the wave train,  $\delta$  is the normalized spectral bandwidth:

$$\varepsilon = a_0 k_0 \quad (1)$$

$$\delta = \frac{\Delta\omega / \omega_0}{\varepsilon}$$

By sweeping through the parameter space, variety of wave groups can be generated. The parameters  $\varepsilon$  and  $\delta$  determines the initial growth rate of the sideband perturbation. According to Benjamin and Feir (1967) the growth rate of the side band is given as:

$$\beta = \varepsilon^2 \delta (2.0 - \delta^2)^{1/2} \quad (2)$$

The growth rate  $\beta$  therefore is approximately proportional to the square of the steepness  $\varepsilon$  and the frequency of the unstable mode is limited in the range  $0 < \delta < 1.4$ . The actual range depends on  $\varepsilon$  as well and the maximum growth rate occurs not at  $\delta=1$  but at lower values for the intermediate values of  $\varepsilon$ . The maximum initial growth condition based on the exact solution by Longuet-Higgins (1980) was compared with that from the Zakharov equation (Krasitskii's coefficients used) and the initial growth rates were experimentally confirmed by Waseda and Tulin (1999).

Long term evolution of the unstable wave train was studied by Melville (1982) who had shown that the instability leads to a formation of a wave group, wave breaking at the peak modulation and the eventual downshifting of the spectrum. A systematic study in the parameter space  $\varepsilon$ - $\delta$  by Tulin and Waseda confirmed Melville's result and showed that the long term evolution for large combinations of  $\varepsilon$  and  $\delta$  led to the wave breaking (Figure 2). The key parameter  $\delta$  is equivalent to the so-called Benjamin-Feir index (Janssen 2003, Onorato et al. 2004):

$$BFI = \sqrt{2\varepsilon} / (2\Delta\omega / \omega_0) \quad (3)$$

or

$$\delta = \frac{1}{\sqrt{2}} \frac{1}{BFI}$$

Therefore, the parameter range  $0.2 < \delta < 1.2$ , for example, will be equivalent to the parameter range  $0.8 < BFI < 5$ . Although the continuous spectral cases of Janssen and Onorato et al. and the 3-wave system studied here are not the same, the latter should serve as a basis for understanding the complex evolution of the former cases. In this presentation, we revisit the earlier study by Tulin and Waseda from the perspective of the rogue wave generation in a wave train.

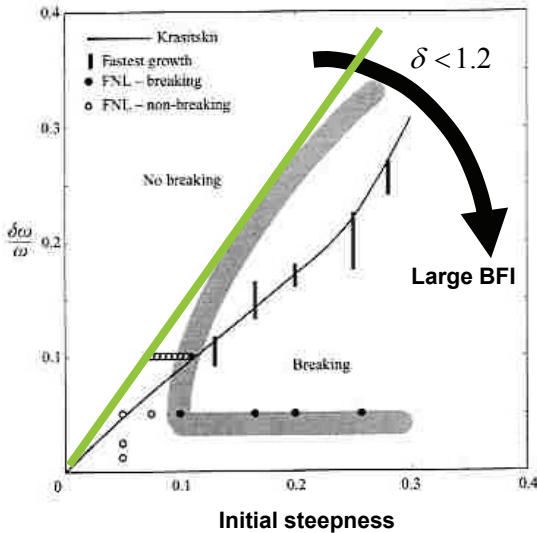


Figure 2: Breaking region in the  $\varepsilon$ - $\delta$  parameter space.

## WEAKLY NONLINEAR EVOLUTION

Numerical solvers of the Dysthe equation (modified nonlinear Schrödinger equation) and the Zakharov equation (in modified form, Krasitskii 1994) will be utilized in this study. The performance of the numerical solvers were compared and verified against fully nonlinear computation in Landrini et al. (2000) and Waseda (1997) and Oshri (1996) describes in more detail the solvers of the Dysthe equation and the Zakharov equation respectively. For both cases, the wave shapes in physical space are obtained numerically. We can then analyze and compare the wave shape with tank experiments.

We have shown that in order to study the long term evolution of the unstable wave train, inclusion of higher frequency free waves in both Dysthe and Zakharov equations are crucial, since the asymmetry of the lower and the upper side band amplitudes at peak modulation results from that. In solving the Dysthe equation, the number of Fourier modes (remainders free from aliasing) can be adjusted by changing

the spatial resolution ( $\Delta x$ ). By gradually reducing the number of free Fourier modes, the long term evolution asymptotically approaches the solution of the cubic NLS and therefore, the contribution from the higher order terms due to broad bandwidth diminishes. Similar experiment can be performed with the Zakharov equation by selectively reducing the active free wave modes. Similar results to the Dysthe equation is obtained; when the number of free wave modes are just three (carrier plus the sidebands), the evolution approaches that of the cubic NLS. In all the results that will be presented here, the parameters of the numeric are selected such that sufficient number of Fourier modes is included to avoid such problem.

## TANK EXPERIMENT

All the unstable wave experiments were conducted with the sideband perturbations seeded to the wave generator motion. Thus, the motion of the wave generator is simply a linear superposition of the three waves, the carrier ( $\omega_0$ ) and the sidebands ( $\omega_{\pm} = \omega_0 \pm \Delta\omega$ ). The initial phases of the three waves are kept constant ( $\phi = 2\alpha - (\beta_+ + \beta_-)$ ) under the condition that the initial sideband amplitudes does not exceed a given threshold. The reason for this is because from the numerical simulation, we have found that the phases of the waves is nearly constant until the sideband amplitudes grows to about 30% of the initial carrier wave amplitude. When the initial sideband amplitude is increased, the total energy is kept constant by reducing the carrier wave amplitude accordingly. The experiments were conducted in this manner, for variety of  $\varepsilon$  and  $\delta$  and the wave records were obtained by wave wire arrays placed along the tank.

## HIGHEST WAVE IN AN UNSTABLE WAVE TRAIN

In the interest of rogue wave generation, we investigate the maximum achievable wave height during the evolution of the unstable wave train. This was first studied experimentally by Su and Green (1982). They have presented the steepness of the maximum wave as a function of the initial steepness of the wave train. The experimental result of Su and Green was compared with the cubic NLS solution by Tanaka (1990). He had shown that the simulation generated much higher maximum wave steepness than the tank experiment. We will show that both studies need to be extended to include wider parameter range. When that is done, the discrepancies between experiment and the weakly nonlinear simulation becomes smaller except for the case when strong nonlinearity should be taken into account, i.e. the cases with wave breaking.

First, the tank experiment is compared with Su's result. Unlike Su's experiment in which the instability occurred naturally, in our experiment the perturbations are all prescribed. For each runs, maximum wave heights are estimated from the wave wire records and are plotted with Su's result (Figure 3). Our results show systematic deviations from Su's and are higher. The scatter of data for different  $\delta$  is apparent as well but within the conducted experimental accuracy we were not able to discern any obvious relationship between maximum wave steepness and  $\delta$ . All the experimental results shown here (blue dots) are cases with wave breaking. Presumably

the experimental ambiguity comes because of that. The same datasets are shown for the enhancement factor (R), which is the ratio of the maximum wave height to the initial wave height (Figure 4). The deviation of our results from Su's is emphasized at the lowest steepness ( $\varepsilon=0.12$ ). As will be shown later, at lower steepness, our experimental result seem to agree better with the weakly nonlinear simulations and therefore casts some question about the validity of Su's experiment below certain steepness. One possible explanation for this is the lack of parameter combinations for Su's experiment in representing the lower steepness cases.

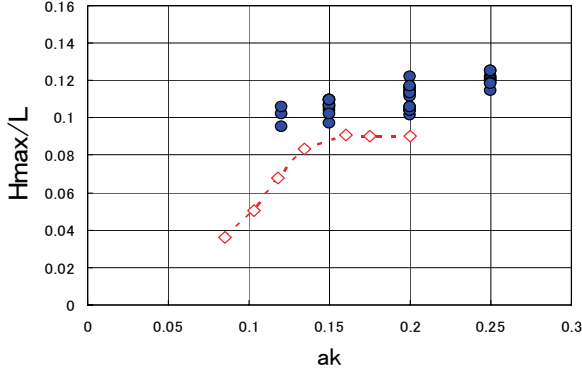


Figure 3: Maximum wave steepness vs. initial steepness. Blue dots: this experiment; red diamonds: Su & Green.

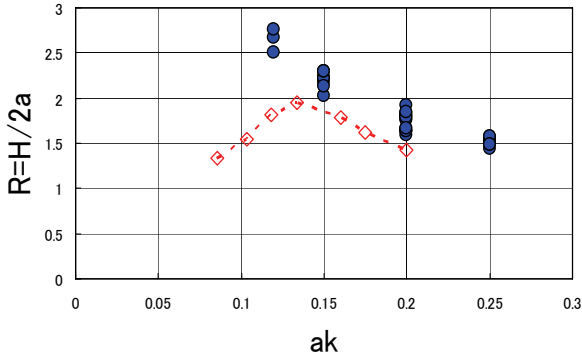


Figure 4: Enhancement factor vs. initial steepness. Blue dots: this experiment; red diamonds: Su & Green.

At lower steepness the evolution of waves become slower and the tank experiment becomes difficult. Tulin and Waseda had shown that below steepness around  $\varepsilon=0.11$  the long term evolution of the unstable wave train does not lead to wave breaking. It is therefore possible to explore the  $\varepsilon$ - $\delta$  space using weakly nonlinear theories below certain steepness. In order also to validate the weakly nonlinear theories we have conducted numerical experiments in the range of  $0.04 < \varepsilon < 0.20$ . Dysthe equation was solved for  $0.4 < \delta < 1.2$  and are plotted in Figure 5 (solid lines) for each  $\delta$ . The result shows the richness of the extreme waves generated in the unstable wave train; a broad range of maximum wave heights are attained for a given steepness. The enhancement factor varies as well (Figure 6) ranging from 1 to 3. The estimations by Dysthe equation are compared with the solution from Zakharov equation (circles) and they agree well in the parameter range studied here. For a given steepness, the maximum wave height is a decreasing function of  $\delta$ . Therefore, for a given steepness, the enhancement of the wave is highest when the

sideband frequencies are closest to that of the carrier wave; i.e. when the spectrum is narrowest. Equivalently, that is to state that the larger the BFI (which is the reciprocal of  $\delta$ ), the larger the maximum wave height. This is consistent with the recent findings by Janssen and Onorato et al., despite the difference in the wave system (3 wave system vs. continuous spectrum).

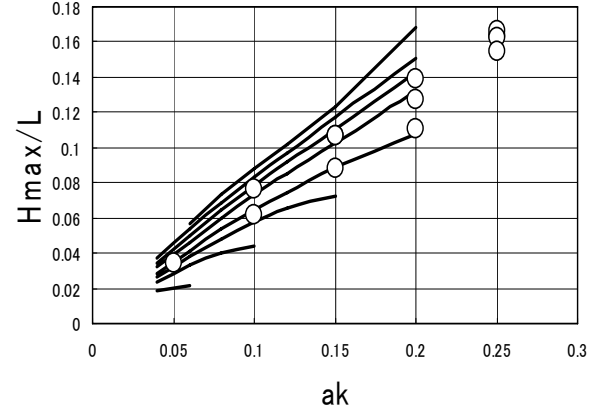


Figure 5: Maximum wave steepness vs. initial steepness. Solid lines: Dysthe equation for different  $\delta$ ; Open circles: Zakharov equation for different  $\delta$ .

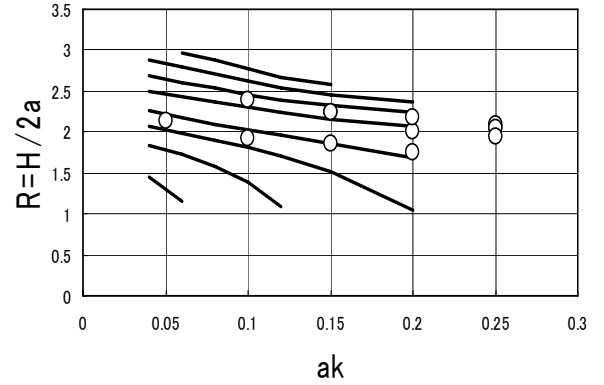


Figure 6: Enhancement factor vs. initial steepness. Solid lines: Dysthe equation for different  $\delta$ ; Open circles: Zakharov equation for different  $\delta$ .

#### HIGHEST WAVE IN A GAUSSIAN SPECTRAL SEA

The study is extended for the evolution of the Gaussian spectral sea. Following Janssen, the Gaussian spectral sea is initialized with random phase; control parameters are  $\varepsilon$  and BFI (or  $\delta$ ).

$$W_{oi} = \frac{BFI}{2\sqrt{\pi}} \exp\left(-\frac{BFI^2}{4\varepsilon^2} p_i^2\right) \left(\frac{\Delta k}{k_0}\right) \quad (4)$$

We present here our preliminary results solving the Zakharov equation for 200 wave periods. Figure 7 is a summary plot of the maximum wave height vs. steepness (which will be explained more in the summary section), and the square symbols are the maximum wave corresponding to different Gaussian spectral sea. For most of the cases, the maximum wave height agreed well with the unstable wave train (3 wave system) for the corresponding  $\varepsilon$  and  $\delta$ . However, for one case at  $\varepsilon=0.15$ , by changing the initial random phase, the maximum wave height exceeded the estimation from the unstable wave train. This indicates that the result from an experiment with just 200 waves is statistically not sufficient and so a large ensemble runs ought to be conducted.

## SUMMARY

Recent tank experimental results had extended the earlier work by Su and Green of the maximum wave in the unstable wave train. The comparison with weakly nonlinear theory (Figure 7) suggests that at steepness higher than certain threshold the waves break and therefore the validity of the weakly nonlinear evolution fails. The steepness of the breaking wave is much smaller than the Stokes limiting value and scatters depending on the wave parameters. It is therefore, not appropriate to discuss the so-called breaking criteria based on the maximum steepness alone and awaits further research. The good agreement comparing the Gaussian spectral sea and the unstable wave train seems to suggest that the knowledge obtained from a simple 3 wave system is useful in assessing the more complicated wave system. Particularly, the suggested upper limit of the maximum wave height due to breaking seems relevant for any wave system and warns the use of weakly nonlinear theory alone in obtaining wave height statistics.

## REFERENCES

- Benjamin, T. B. and J. E. Feir, 1967, The disintegration of wavetrains on deep water, *J. Fluid Mech.*, **27**, 417-430.
- Janssen PAEM, 2003, Nonlinear four-wave interactions and freak waves, *J. Phys. Oceanogr.*, **33** (4): 863-884
- Krasitskii, V.P. 1994, On reduced equations in the Hamiltonian theory of weakly nonlinear surface waves, *J. Fluid Mech.*, **272**, 1 – 20
- Landrini, M., O. Oshri, T. Waseda, and M. P. Tulin., 1998, Long-time evolution of gravity wave systems. In: Proceedings 13<sup>th</sup> International Workshop on Water Waves and Floating Bodies, Alphen aan den Rijn, The Netherlands.

- Longuet-Higgins, M. S., 1980, Modulation of the amplitude of steep wind waves, *J. Fluid Mech.*, **99**, 705-713
- Melville, W. K., 1982, The instability and breaking of deep-water waves, *J. Fluid Mech.*, **115**, 165 - 185
- Onorato, M., A. R. Osborne, M. Serio, L. Cavaleri, C. Brandini, C.T. Stansberg, 2004, Observation of strongly non-Gaussian statistics for random sea surface gravity waves in wave flume experiments, *Phys. Review E.*, Vol 70, 067302, pp. 1-4.
- Oshri, O., 1996, Frequency downshifting in surface waves and free surface flows without waves, *Ph.D thesis, U. of California at Santa Barbara* Waseda,
- Su M.-Y, Green A. W., 1984, Coupled Two-dimensional and 3-dimensional instabilities of surface gravity-waves, *Physics of fluids*, **27** (11): 2595-2597
- Tanaka, M., 1990, Maximum amplitude of modulated wave train, *Wave Motion*, **12**, 559-568
- Ten I. and H. Tomita, 2005, Creation and Annihilation of Extremely Steep Transient Wave, the Proceedings of the Fifteenth International Offshore and polar engineering conference, Vol. III, 10-17
- Tulin, M. P. and T. Waseda, 1999, Laboratory observations of wave group evolution, including breaking effects, *J. Fluid Mech.*, **378**, 197-232
- Waseda, T., 1997, Laboratory study of wind and mechanically generated wave, *Ph.D thesis, U. of California at Santa Barbara*
- Waseda, T. and M. P. Tulin (1999), 'Experimental study of the stability of deep-water wave trains including wind effects', *J. Fluid Mech.*, **401**, 55-84
- Waseda, T., C.-K. Rheem, J. Sawamura, T. Yuhara, T. Kinoshita, K. Tanizawa and H. Tomita, 2005, Extreme Wave Generation in Laboratory Wave Tank, the Proceedings of the Fifteenth International Offshore and polar engineering conference, Vol. III, 1-9

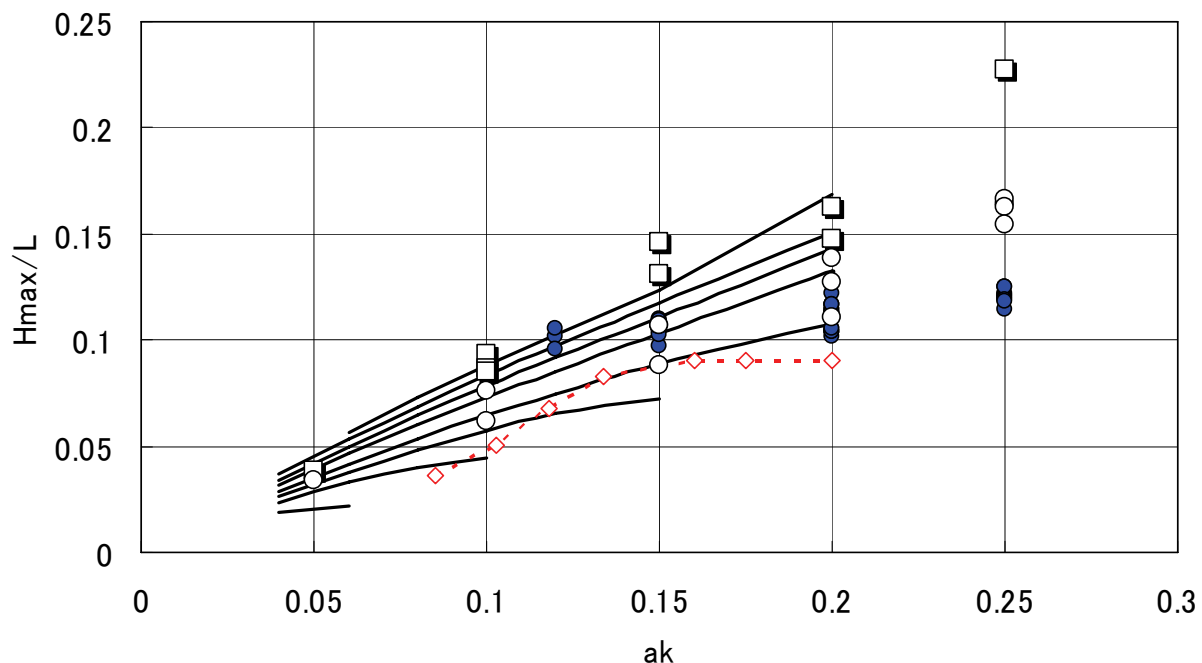


Figure 7: Maximum wave steepness vs. initial steepness. Blue dots: this experiment; red diamonds: Su & Green experiment; Solid lines: Dysthe equation for different  $\delta$ ; Open circles: Zakharov equation for different  $\delta$ ; Open square: Zakharov equation for Gaussian sea